nature research

https://doi.org/10.1038/s41929-020-00518-5

Supplementary information

Microwave-initiated catalytic deconstruction of plastic waste into hydrogen and high-value carbons

In the format provided by the authors and unedited

Supplementary Information for

Microwave-initiated Catalytic Deconstruction of Plastic Waste into Hydrogen and High-Value Carbons

Xiangyu Jie[1], Weisong Li[1, 2, 3], Daniel Slocombe[4], Yige Gao[1], Ira Banerjee[1], Sergio Gonzalez-Cortes[1], Benzhen Yao[1], Hamid AlMegren[5], Saeed Alshihri[5], Jonathan Dilworth[1], John Thomas[6*], Tiancun Xiao[1*] and Peter Edwards[1*]

1. Inorganic Chemistry Laboratory, Department of Chemistry, University of Oxford, South Parks Road, Oxford OX1 3QR, UK

2. School of Chemical Engineering and Technology, China University of Mining and Technology, Xuzhou, 221116, China

3. School of Chemical Engineering and Technology, Tianjin University, Tianjin, 300350, China

4. School of Engineering, Cardiff University, Queen's Buildings, The Parade, Cardiff, CF24 3AA, UK

5. Materials Division, King Abdulaziz City for Science and Technology, Riyadh 11442, Kingdom of Saudi Arabia

6. Department of Materials Science and Metallurgy, University of Cambridge, 27 Charles Babbage Road, Cambridge, CB3 0FS, UK.

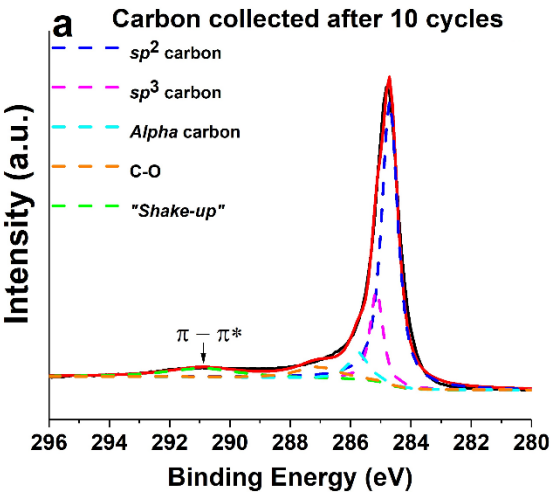

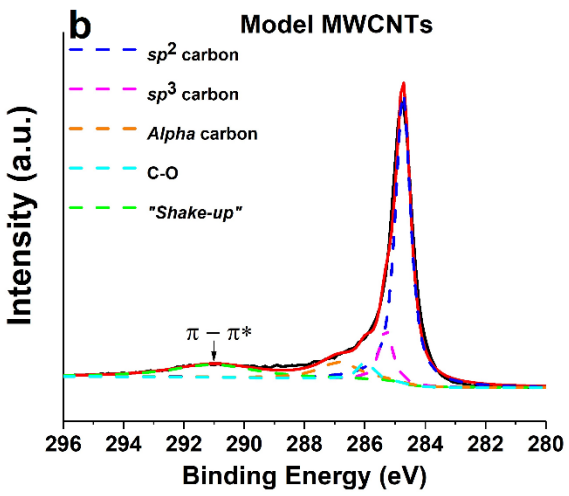

Carbon collected after 10 cycles	Position (eV)	FWHM (eV)	Area (a.u.)	Percentage (%)
sp^2 carbon	284.7	0.635	47727	62.13
sp^3 carbon	285.1	0.488	11980	15.59
Alpha carbon	285.7	0.747	5375.9	6.99
C-O	287.1	1.660	5148.3	6.70
Shake-up	290.9	2.789	6590.7	8.58

Model MWCNTs	Position (eV)	FWHM (eV)	Area (a.u.)	Percentage (%)
sp^2 carbon	284.7	0.599	19822.9	62.08
sp^3 carbon	285.3	0.529	3140.2	9.83
Alpha carbon	285.9	0.595	1238.1	3.88
C-O	286.9	1.551	2987.2	9.36
Shake-up	291.0	3.284	4737.9	14.84

Supplementary Fig. 1: XPS analysis of **(a)** carbon collected after 10 cycle and **(b)** model MWCNTs. The contribution of each carbon type to the experimental spectra is fit in the dash lines. As observed, sp^2 and sp^3 carbon atoms are dominant in both samples with the sharp peaks centred at 284.7 and 285.2 eV, respectively. The characteristic shake-up line of carbon in π – π* transition is observed at ca. 290.9 eV[1,2] in both samples, suggesting the produced carbon is primarily MWCNTs.

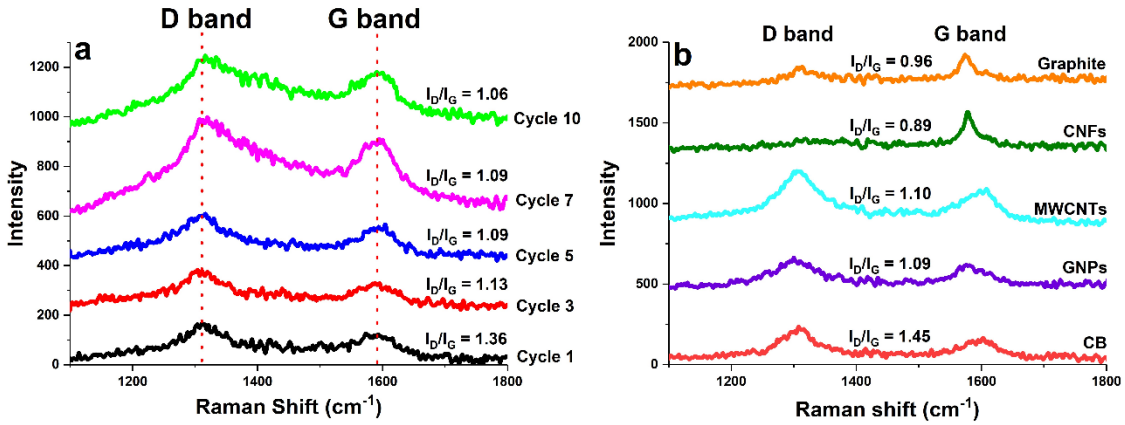

Supplementary Fig. 2: Raman spectrum. **(a)** Resulting carbons throughout 10 successive cycles of HDPE decomposition using $FeAlO_x$ catalysts. The Raman spectroscopy reveals characteristic D-band and G-band at around 1318 cm^{-1} and 1590 cm^{-1}, respectively. **(b)** Model carbon materials. Compared to the I_D/I_G of model carbon materials, the produced carbon has an I_D/I_G value ranging from 1.06 to 1.13 (except cycle 1) that is very close to MWCNTs and GNPs, indicating the formation of carbon in aromatic ring structure and it is a fair assumption that the produced carbon is primarily MWCNTs. In comparison, I_D/I_G of sample after cycle 1 is 1.36 which is ascribed to the presence of other forms of carbon such as carbon black etc.

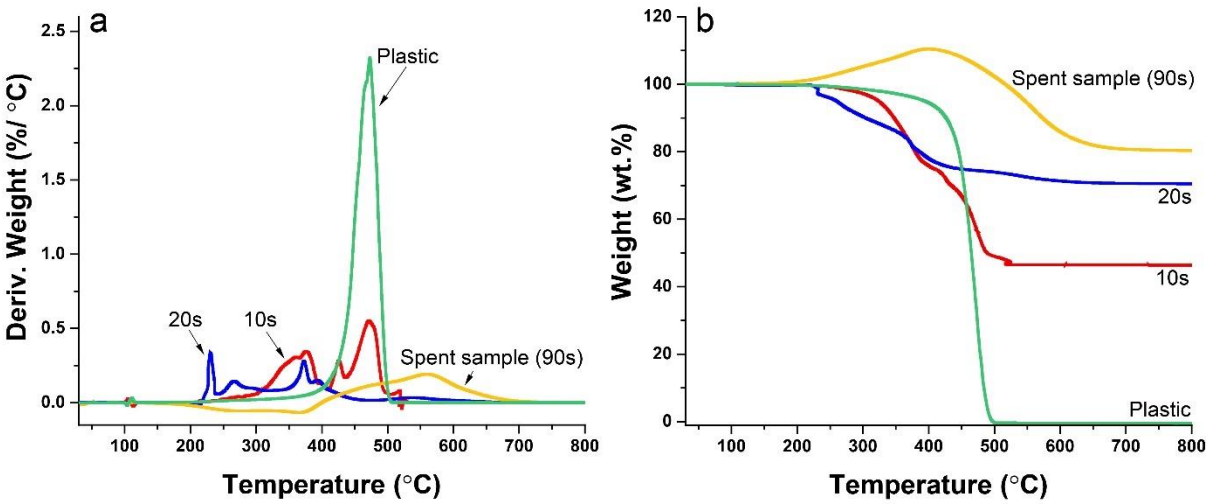

Supplementary Fig. 3: Thermogravimetric analysis (TGA) of representative spent $FeAlO_x$ catalysts. (a) Derivative plots of temperature programmed oxidation (TPO). **(b)** Weight loss. The labelled 10s and 20s are the sample exposed to microwave irradiation for 10 and 20s, respectively. The plastic here is HDPE and presented as a reference. Peaks other than plastic obtained in the sample of 10s and 20s at lower temperature indicate the production of intermediates in the reactions. These corresponding to the weight loss observed in (b). No such compounds are found in the spent sample.

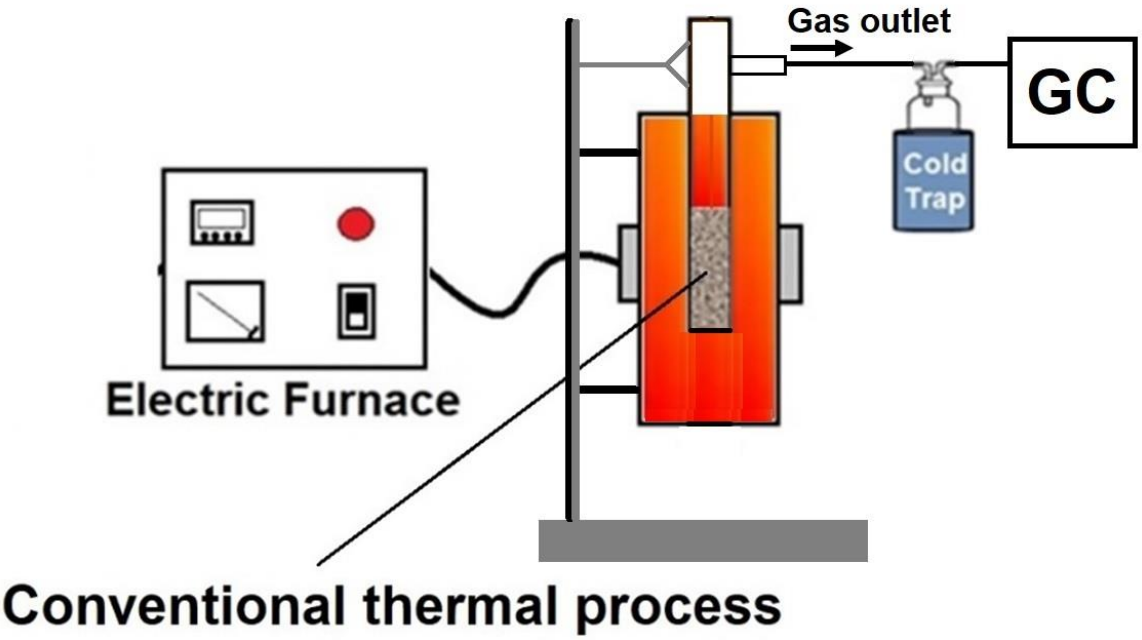

Supplementary Fig. 4: A conventional thermal system configuration, heating by an electric furnace.

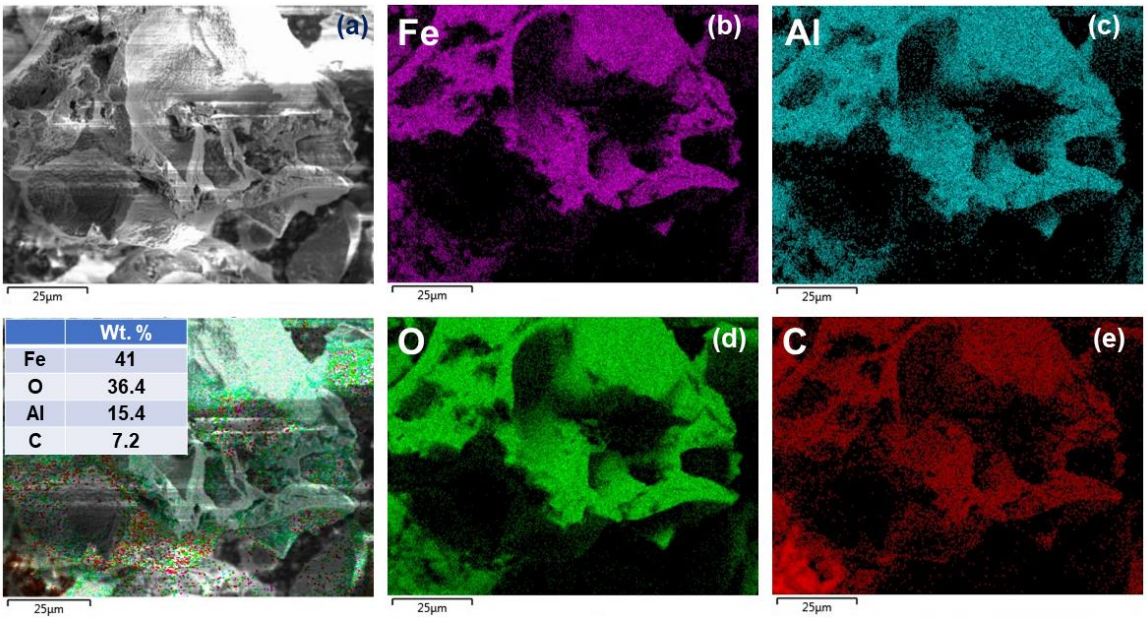

Supplementary Fig. 5: Energy-dispersive X-ray spectroscopy (EDS) mapping of the elemental species on the surface of fresh $FeAlO_x$ catalysts before microwave activation. (A) SEM (backscattered electron) morphology, (B) Fe map, (C) Al map, (D) O map, and (E) C map.

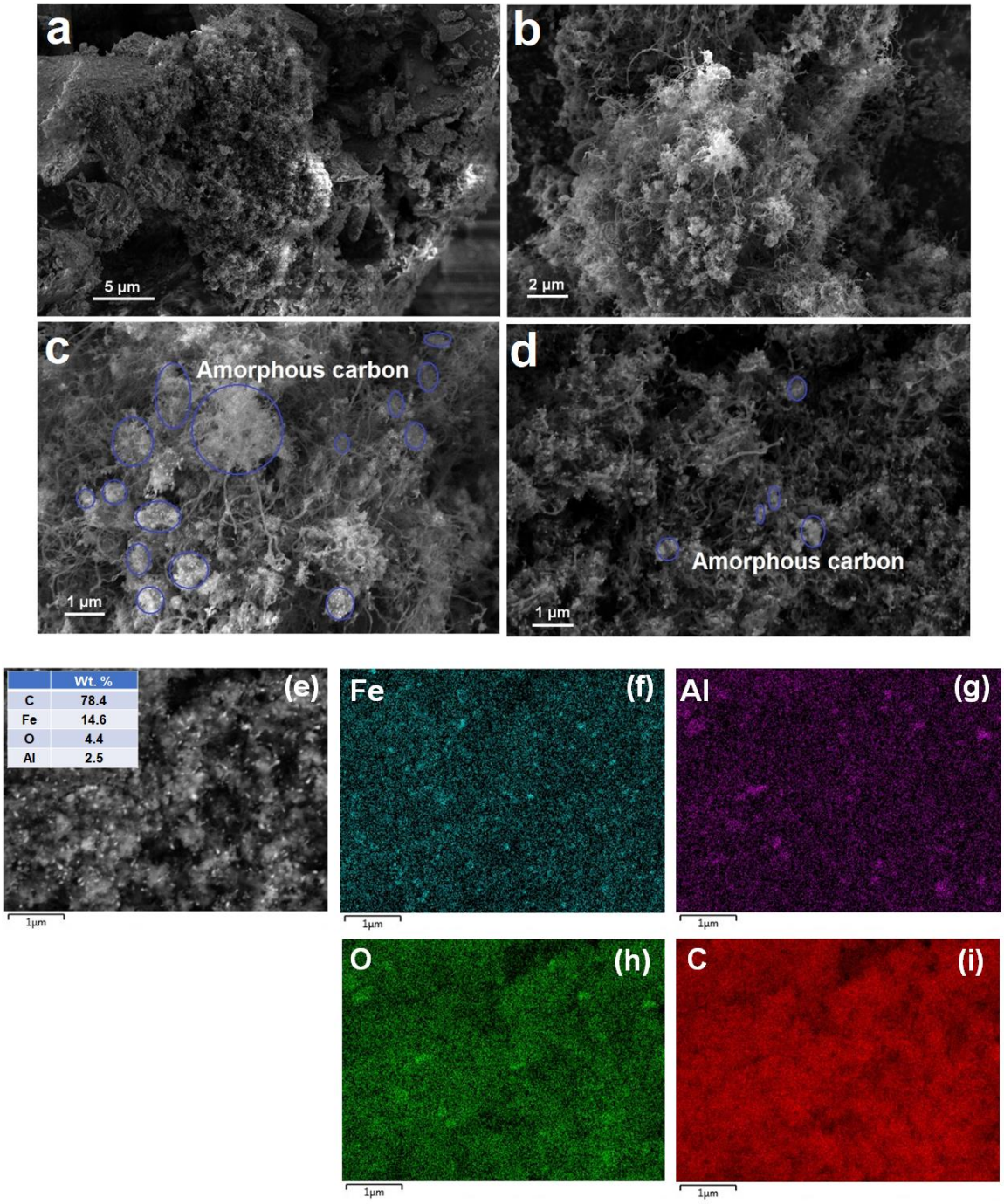

Supplementary Fig. 6: (a-d) Scanning electron microscope (SEM) images and **(e-i)** Energy-dispersive X-ray spectroscopy (EDS) mapping of the elemental species on the surface of spent $FeAlO_x$ catalysts after first cycle of decomposition of high-density polyethylene (HDPE). **(c, d)** Some amorphous carbon observed was highlighted in blue circles. **(e)** SEM (backscattered electron) morphology, **(f)** Fe map, **(g)** Al map, **(h)** O map, and **(i)** C map. Unlike the samples of cycle 10 (Supplementary Fig 6) which were almost covered by carbon, active Fe and other elements such as O and Al were also detected in cycle 1.

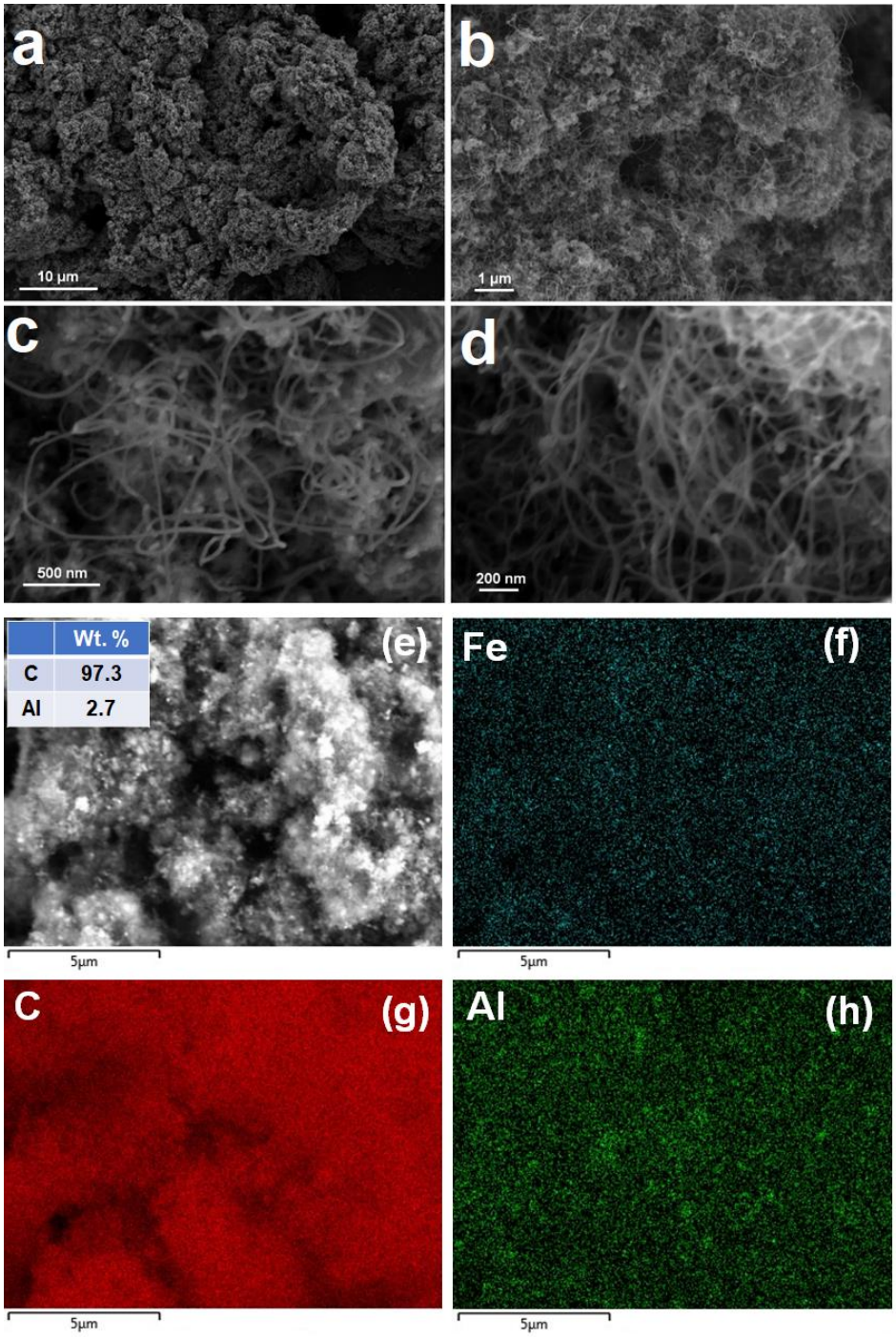

Supplementary Fig. 7: (a-d) Scanning electron microscope (SEM) images and **(e-h)** Energy-dispersive X-ray spectroscopy (EDS) mapping of the elemental species on the surface of spent $FeAlO_x$ catalysts after 10 successive cycles of decomposition of high-density polyethylene (HDPE). **(c, d)** As a general observation, the produced carbon nano-materials were grown as bulks of filamentous carbon clusters. **(e)** SEM (backscattered electron) morphology, **(f)** Fe map, **(g)** C map and **(h)** Al map. Nearly only MWCNTs was observed after 10 cycles.

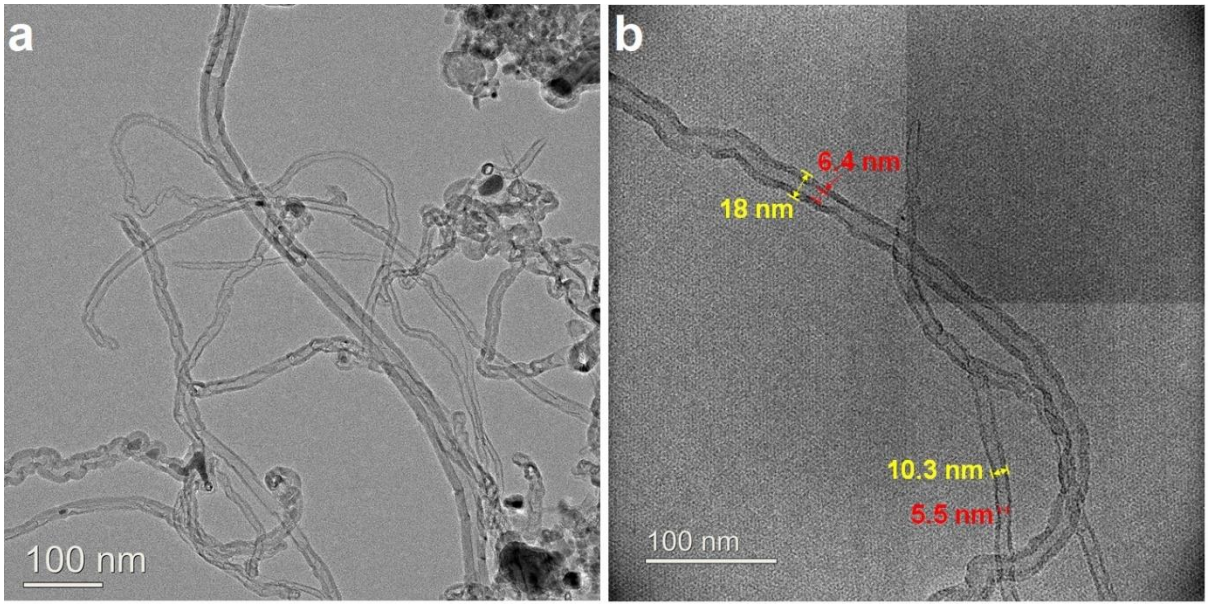

Supplementary Fig. 8: Transmission electron microscopy (TEM) images of produced carbon nanotubes in spent samples after 10 successive cycles of decomposition of high-density polyethylene (HDPE). The formed MWCNTs has outer diameters of ca. 20 nm, with inner diameters of ca. 6 nm.

Supplementary Table 1: Experimental results for the microwave-driven decomposition of high-density polyethylene (HDPE) using different microwave susceptor catalysts.

	Fe	Fe_2O_3	Fe_3O_4	Fe_3C	Ni	Co	Co_3O_4	$FeNiAlO_x$ (1:1:1:1) *	$FeCoAlO_x$ (1:1:1:1) *
Evolved gas composition (Vol. %)									
H_2	42.9	61.3	69.5	39.7	22.3	71.2	64.0	72.7	73.3
CH_4	20.8	3.4	4.6	19.9	23.8	8.2	4.8	13.1	4.2
C_{2+}	33.7	7.6	4.0	38.9	50.8	18.5	7.1	3.1	3.2
CO	2.2	24.5	20.5	1.3	2.9	1.9	20.5	9.1	17.1
CO_2	0.4	3.1	1.4	0.2	0.3	0.2	3.6	2.0	2.1
H_2 yield (mmol· $g_{plastic}^{-1}$)	9.0	19.1	29.7	4.0	3.0	17.1	35.1	23.6	34.1
Gas yield (wt.%)	33.0	39.1	41.8	16.9	28.3	22.9	64.4	25.8	41.7
Solid yield (wt.%)	54.8	54.8	54.8	54.8	37.9	71.1	31.3	78.1	53.9
Oil yield (wt.%)	12.2	6.1	3.4	28.3	33.8	5.9	4.3	(-)	4.4
Mass balance (%)	87.8	93.9	96.6	71.7	66.2	94.1	95.7	103.9	95.6

* The numbers in parentheses refer to the mole ratio of Fe:Ni/Co:Al:citric acid.

Supplementary Table 2: Experimental results for the microwave-driven decomposition of high-density polyethylene (HDPE) using different supported Fe-based microwave susceptor catalysts and also different carbon materials.

	Fe/AC[§]	Fe/SiC[§]	Fe/Al_2O_3[§]	Fe/ZSM-5 (Si/Al=46) [§]	AC[*]	GNPs[*]	Graphite
Evolved gas composition (Vol. %)							
H_2	62.3	42.1	53.1	42.6	51.2	50.8	28.2
CH_4	20.7	24.5	18.5	12.9	24.1	30.4	27.3
C_{2+}	9.6	31.1	24.4	43.2	21.4	13.8	42.5
CO	7.2	2.3	3.9	1.2	2.6	4.4	1.4
CO_2	0.2	0.1	0.1	0.2	0.8	0.6	0.6
H_2 yield (mmol·$g^{-1}_{plastic}$)	23.2	4.2	12.9	11.6	5.7	8.3	4.3
Gas yield (wt.%)	36.3	14.8	31.0	51.5	14.8	19.3	29.1
Solid yield (wt.%)	49.0	64.5	53.0	22.5	5.8	65.6	66.2
Oil yield (wt.%)	14.7	20.7	16	25.9	37.7	15.1	4.8
Mass balance (%)	85.3	79.3	84.0	74.1	62.3	84.9	95.2

[§] The Fe loading for all the supported Fe catalysts are 40 wt.%.

* ACs refers to activated carbons and GNPs refers to graphene nanoplatelets.

┼ MWCNTs had been also tested for HDPE decomposition under microwave irradiation. Unfortunately, no reaction was observed over MWCNTs.

Supplementary Table 3: Experimental results for 5 successive cycles of the microwave-driven decomposition of milk bottles (High density polyethylene, HDPE) using $FeAlO_x$ catalysts.

	Cycle 1	Cycle 2	Cycle 3	Cycle 4	Cycle 5
Evolved gas composition (Vol. %)					
H_2	74.3	88.0	83.1	82.6	78.4
CH_4	5.8	5.0	7.8	8.1	5.9
C_{2+}	2.8	0.9	3.4	3.5	10.4
CO	15.2	5.3	5.1	5.2	4.9
CO_2	1.8	0.9	0.5	0.6	0.4
H_2 yield (mmol·$g_{plastic}^{-1}$)	55.6	50.5	40.4	38.8	35.0
Gas yield (wt.%)	62.7	27.3	28.4	28.0	34.2
Solid yield (wt.%)	35.1	73.1	72.0	68.1	63.1
Oil yield (wt.%)	2.2	(-)	(-)	3.9	2.6
Mass balance (%)	97.8	100.4	100.4	96.1	97.4

Supplementary Table 4: Experimental results for 5 successive cycles of the microwave-driven decomposition of waste packaging (polypropylene, PP) using $FeAlO_x$ catalysts.

	Cycle 1	Cycle 2	Cycle 3	Cycle 4	Cycle 5
Evolved gas composition (Vol. %)					
H_2	73.7	81.5	81.8	78.2	77.0
CH_4	7.4	6.4	11.9	7.8	9.6
C_{2+}	3.4	1.7	0.9	9.3	9.8
CO	14.2	9.6	4.8	4.4	3.4
CO_2	1.3	0.8	0.7	0.2	0.1
H_2 yield (mmol·$g_{plastic}^{-1}$)	50.2	51.4	45.6	40.3	40.1
Gas yield (wt.%)	57.3	39.1	30.4	39.3	40.1
Solid yield (wt.%)	36.3	60.4	65.4	57.8	54.3
Oil yield (wt.%)*	6.4	0.5	4.2	2.9	5.5
Mass balance (%)	93.6	99.5	95.8	97.1	94.5

Supplementary Table 5: Experimental results for 5 successive cycles of the microwave-driven decomposition of waste plastic foam (polystyrene, PS) using $FeAlO_x$ catalysts.

	Cycle 1	Cycle 2	Cycle 3	Cycle 4	Cycle 5
Evolved gas composition (Vol. %)					
H_2	76.1	81.3	82.9	82.7	81.0
CH_4	7.8	6.4	6.7	6.7	7.7
C_{2+}	2.2	1.8	1.6	1.8	2.3
CO	12.5	9.6	8.2	8.1	8.3
CO_2	1.4	0.9	0.5	0.7	0.7
H_2 yield (mmol·$g_{plastic}^{-1}$)	23.1	20.4	24.5	22.4	26.9
Gas yield (wt.%)	22.9	15.7	16.9	15.7	20.4
Solid yield (wt.%)	75.9	83.3	79.6	81.7	75.2
Oil yield (wt.%)	1.2	1.1	3.5	2.5	4.4
Mass balance (%)	98.8	98.9	96.5	97.5	95.6

Supplementary Table 6: Experimental results for the microwave-driven decomposition of waste plastic mixtures using $FeAlO_x$ catalysts.

PE:PP:PS (wt.%)	Evolved gas composition (Vol.%)					H_2 yield (mmol· $g_{plastic}^{-1}$)	Gas yield (wt.%)	Solid yield (wt.%)	Oil yield (wt.%)	Mass balance (%)
	H_2	CH_4	C_{2+}	CO	CO_2					
90:5:5	66.4	6.0	7.0	18.8	1.8	36.7	58.5	40.3	1.1	98.9
75:20:5	71.8	4.4	5.0	16.8	2.0	39.0	51.2	58.0	(-)	109.2
45:45:10	73.4	4.2	4.2	16.4	1.8	36.1	44.1	59.7	(-)	103.7
20:75:5	73.1	7.9	5.4	11.2	2.5	41.3	50.7	49.9	(-)	100.5
25:25:50	75.2	7.6	2.4	12.9	1.8	30.7	32.5	61.8	5.7	94.3
Waste PE plastic bags	75.8	4.0	4.0	14.7	1.5	47.3	51.3	45.4	3.3	96.7

Supplementary Table 7: Comparison of catalytic performance of hydrogen production from plastic waste with other methods.

Type of Reactor	Catalyst	Type of plastic	Temp. (°C)	Steam (Y/N)	Evolved gas composition (Vol.%)					H_2 yield (mmol·$g^{-1}_{plastic}$)	Gas yield (wt.%)	Solid yield (wt.%)	Oil yield (wt.%)	Ref.
					H_2	CH_4	C_{2+}	CO	CO_2					
Microwave reactor	$FeAlO_x$	Real-world waste plastics	300 – 380	No	74.3	5.8	2.8	15.2	1.8	55.5	62.7	35.1	2.2	**This work**
					88.0	5.0	0.9	5.3	0.9	50.5	27.3	73.1	(-)	
					83.1	7.8	3.4	5.1	0.5	40.5	28.4	72.0	(-)	
					82.6	8.1	3.5	5.2	0.6	39	28.0	68.1	3.9	
					78.4	5.9	10.4	4.9	0.4	35	34.2	63.1	2.6	
Two-stage fixed bed reactor	Sand	Real-world waste plastics	800	No	24.7	49.4	22.3	3.0	0.7	8	50.5	2.2	27.8	3
	$Ni/\gamma\text{-}Al_2O_3$				52.6	39.6	1.9	4.5	1.4	22.5	41.8	21.1	36.4	
	$Ni/\alpha\text{-}Al_2O_3$				48.4	41.1	4.0	5.5	0.9	18	39.6	26.1	37.8	
	$Fe/\gamma\text{-}Al_2O_3$				57.5	35.8	1.4	4.6	0.7	23	35.3	32.6	36.2	
	$Fe/\alpha\text{-}Al_2O_3$				57.6	34.1	2.8	4.8	0.6	20.5	32.4	35.2	32.5	
	$Ni\text{-}Fe/\gamma\text{-}Al_2O_3$				62.9	27.2	2.7	6.2	1.0	32	43.0	40.7	19.6	
	$Ni\text{-}Fe/\gamma\text{-}Al_2O_3$			Yes S/P=2.6*	62.9	6.6	0.9	28.1	1.6	92.5	164.4	3.5	120.1	
	$Ni\text{-}Fe/\gamma\text{-}Al_2O_3$		700	No	66.5	21.4	5.7	5.2	1.1	27	34.1	43.2	23.8	
	$Ni\text{-}Fe/\gamma\text{-}Al_2O_3$		900		72.2	20.8	0.2	6.0	0.8	43.5	41.6	44.0	16.8	

Two-stage fixed bed reactor	Ni–Mn–Al catalyst	Real-world waste plastics	800	No	76.6	15.9	0.2	6.9	0.4	14	46.1	48.0		4
	Ni–Mn–Al catalyst		800	Yes	63.4	7.4	0.3	24.1	4.8	23.5	170.1	19.0		
Two-stage fixed bed reactor	Ni Al_2O_3	LDPE	800	No	36.6	23.6	39.8				61.2	26.6	12.2	5
	Fe Al_2O_3				50.6	19.8	29.6				55.7	18.4	26.0	
	Co Al_2O_3				31.3	24.9	43.8				60.2	29.8	9.9	
	Cu Al_2O_3				26.0	26.6	47.4				60.4	31.9	7.7	
Two-stage fixed bed reactor	Fe-SiO2-S	PP	800	No	41.7	39.1	13.8	5.3		15.4	49.2	26		6
	Fe-SiO2-L				50.3	22.7	19.2	7.8		25.6	63.9	29		
	Ni-SiO2-S				42.2	43.5	11	3.3		18.1	51.2	16		
	Ni-SiO2-L				47.7	38.3	7.6	6.3		22.6	52.5	16		
Two-stage fixed bed reactor	Ru/γ−Al_2O_3	PS	580	Yes	69.2			5.2	24.9	130				7
	Ru/γ−Al_2O_3		680		68.3			10.2	21.1	159				
Two-stage fixed bed reactor	Ni–Zn–Al	PP	800	Yes	52.7	13.4	9.4	19.5	5.0	46	120.9	10.0		8
	Ni–Mg–Al				56.9	9.8	2.8	26.9	3.5	75.5	168.4	3.5		
	Ni–Ca–Al				58.3	9.4	4.3	23.7	4.4	68.5	148.2	9.5		
	Ni–Ce–Al				55.6	10.6	5.0	24.9	3.9	63	148.6	8.0		
	Ni–Mn–Al				62.7	9.2	1.8	20.9	5.4	71.5	131.1	23.0		
Two-stage fixed bed reactor	NiMnAl444	PP	800	Yes	75.6	12.7	1.6	9.1	1.0	37.2	34.6	57.7	6.3	9
	NiMnAl424				70.8	9.6	0.4	16.6	2.7	56.6	71.2	46.6	7.0	

* S/P: Steam to plastic ratio

Supplementary Table 8: Experimental results for the microwave-driven decomposition of high-density polyethylene (HDPE) using $FeAlO_x$ catalysts which had been prepared by varying the molar ratio of Fe/Al/citric acid.

Molar ratio†	**10:1:1**	**10:5:1**	**10:5:5**	**10:8:2**	**10:8:10**	**10:10:10**	**10:10:5**	**10:14:5**	**10:21:5**
Evolved gas composition (Vol. %)									
H_2	64.0	54.1	66.2	72.8	71.4	74.3	77.6	71.1	62.2
CH_4	2.2	9.2	10.3	5.9	11.1	5.8	4.2	6.9	10.9
C_{2+}	2.3	20.5	12.0	2.9	5.8	2.8	6.1	6.8	8.3
CO	29.0	15.4	10.7	16.5	10.6	15.2	11.8	13.2	16.8
CO_2	2.5	0.8	0.8	1.9	1.1	1.8	0.4	1.9	1.7
H_2 yield (mmol·$g^{-1}_{plastic}$)	40.7	20.8	34.9	40.9	45.7	55.6	23.8	25.3	18.3
Gas yield (wt.%)	74.0	53.1	53.5	49.5	55.9	62.7	23.7	32.9	32.5
Solid yield (wt.%)	20.5	47.2	46.6	58.4	35.1	35.1	68.3	68.2	74.0
Oil yield (wt.%)	5.6	(-)	(-)	(-)	8.9	2.2	8.0	(-)	(-)
Mass balance (%)	94.4	100.3	100.1	107.9	91.1	97.8	92.0	101.1	106.6

† The molar ratio indicates the molar ratio of Fe:Al:citric acid, and also gives the amount of $Fe(NO_3)_3 \cdot 9H_2O$, $Al(NO_3)_3 \cdot 9H_2O$ and citric acid used when preparing the catalysts.

Supplementary Table 9: Comparison of microwave and conventional thermal decomposition of HDPE using $FeAlO_x$ catalysts. The temperature used for thermal experiments were 550 °C and the highest temperature recorded under microwave was ca. 350 °C.

	Thermal	**Microwave**
Evolved gas composition (Vol. %)		
H_2	40.7	74.3
CH_4	14.5	5.8
C_{2+}	37.8	2.8
CO	2.6	15.2
CO_2	4.4	1.8
H_2 yield (mmol·$g_{plastic}^{-1}$)	4.3	55.6
Gas yield (wt.%)	21.8	62.7
Solid yield (wt.%)	12.3	35.1
Oil yield (wt.%)	66.0	2.2

Supplementary Table 10: Experimental results for the microwave-driven decomposition of HDPE using FeAlOx catalysts with different starting weight ratio of HDPE and $FeAlO_x$ catalysts.

Weight ratio (HDPE: Catalysts)	Evolved gas composition (Vol.%)					H_2 yield (mmol· $g^{-1}_{plastic}$)	Gas yield (wt.%)	Solid yield (wt.%)	Oil yield (wt.%)	Mass balance (%)
	H_2	CH_4	C_{2+}	CO	CO_2					
0.3:1	68.1	3.4	2.1	22.1	4.3	45.5	71.4	32.3	(-)	103.7
1:1	74.3	5.8	2.8	15.2	1.8	55.6	62.7	35.1	2.2	97.8
2:1	72.0	2.8	0.6	23.0	1.6	50.3	64.2	37.7	(-)	102.0
3:1	70.0	7.2	11.2	11.2	0.3	35.2	50.2	45.1	4.7	95.3
5:1	69.1	5.0	6.0	17.8	2.2	25.1	36.6	49.6	13.8	86.2
>10:1 *						(-)				

* by the mixing weight ratio (HDPE : $FeAlO_x$ catalysts) over 10, negligible gas was produced and instead, waxes are produced.

Supplementary Table 11: Experimental results for 10 successive cycles of the microwave-driven decomposition of milk bottles (High density polyethylene, HDPE) using $FeAlO_x$ catalysts.

	Evolved gas composition (Vol.%)					H_2 yield (mmol· $g_{plastic}^{-1}$)	Gas yield (wt.%)	Solid yield (wt.%)	Oil yield (wt.%)	Mass balance (%)
	H_2	CH_4	C_{2+}	CO	CO_2					
Cycle 1	74.3	5.8	2.8	15.2	1.8	55.6	62.7	35.1	2.2	97.8
Cycle 2	88.0	5.0	0.9	5.3	0.9	50.5	27.3	73.1	(-)	100.4
Cycle 3	83.1	7.8	3.4	5.1	0.5	40.4	28.4	72.0	(-)	100.4
Cycle 4	82.6	8.1	3.5	5.2	0.6	38.8	28.0	68.1	3.9	96.1
Cycle 5	78.4	5.9	10.4	4.9	0.4	35.0	34.2	63.1	2.6	97.4
Cycle 6	76.7	9.8	9.2	3.9	0.3	34.1	32.6	66.2	1.2	98.8
Cycle 7	65.7	17.1	14.8	2.3	0.1	21.1	30.3	64.7	4.9	95.1
Cycle 8	61.5	18.8	16.8	2.7	0.1	18.4	30.5	64.2	5.3	94.7
Cycle 9	52.6	21.9	23.5	1.8	0.2	15.1	35.7	57.6	6.7	93.3
Cycle 10	41.6	27.3	28.7	2.3	0.1	8.9	31.8	63.7	4.4	95.6

Supplementary References:

1 Zhang, Y. *et al.* Kinetics and interfacial thermodynamics of the pH-related sorption of tetrabromobisphenol A onto multiwalled carbon nanotubes. *ACS APPL MATER INTER* **6**, 20968-20977 (2014).

2 Munaiah, Y., Suresh, S., Dheenadayalan, S., Pillai, V. K., Ragupathy, P. Comparative Electrocatalytic performance of single-walled and multiwalled carbon nanotubes for zinc bromine redox flow batteries. *J. Phys. Chem. C* **118**, 14795-14804 (2014).

3 Yao, D., Zhang, Y., Williams, P. T., Yang, H. & Chen, H. Co-production of hydrogen and carbon nanotubes from real-world waste plastics: Influence of catalyst composition and operational parameters. *Appl. Catal. B-Environ.* **221**, 584-597 (2018).

4 Wu, C., Nahil, M. A., Miskolczi, N., Huang, J., Williams, P. T. Processing real-world waste plastics by pyrolysis-reforming for hydrogen and high-value carbon nanotubes. *Environ. Sci.* **48**, 819-826 (2013).

5 Acomb, J. C., Wu, C., Williams, P. T. The use of different metal catalysts for the simultaneous production of carbon nanotubes and hydrogen from pyrolysis of plastic feedstocks. *Appl. Catal. B-Environ.* **180**, 497-510 (2016).

6 Liu, X., Zhang, Y., Nahil, M. A., Williams, P. T., Wu, C. Development of Ni- and Fe-based catalysts with different metal particle sizes for the production of carbon nanotubes and hydrogen from thermo-chemical conversion of waste plastics. *J Anal Appl Pyrolysis* **125**, 32-39 (2017).

7 Namioka, T. *et al.* Hydrogen-rich gas production from waste plastics by pyrolysis and low-temperature steam reforming over a ruthenium catalyst. *Appl. Energy* **88**, 2019-2026 (2011).

8 Nahil, M. A., Wu, C., Williams, P. T. Influence of metal addition to Ni-based catalysts for the co-production of carbon nanotubes and hydrogen from the thermal processing of waste polypropylene. *Fuel Process. technol.* **130**, 46-53 (2015).

9 Wu, C., Nahil, M. A., Huang, J., Williams, P. T. Production and application of carbon nanotubes, as a co-product of hydrogen from the pyrolysis-catalytic reforming of waste plastic. *PROCESS SAF ENVIRON* **103**, 107-114 (2016).